

ECOPHYSIOLOGY AND PHYTOREMEDIATION POTENTIAL OF HEAVY METAL(LOID) ACCUMULATING PLANTS

ANTHONY GEORGE KACHENKO

B.Hort.Sc.(Hons)

A THESIS SUBMITTED IN FULFILMENT OF THE REQUIREMENTS
FOR THE DEGREE OF DOCTOR OF PHILOSOPHY

Faculty of Agriculture Food and Natural Resources
The University of Sydney
New South Wales
Australia

— MMVIII —

— CERTIFICATE OF ORIGINALITY —

I hereby declare that the text of this thesis is my own work, and that, to the best of my knowledge and belief, it contains no material that has been previously published or written by another person, nor any material that has been accepted as part of the requirements for any other degree or diploma in any university or other institute of higher learning, unless due acknowledgement has been made.

I also declare that the intellectual content of this thesis is original and the result of my own research and to the best of my knowledge and belief, any assistance I received in the experimentation presented, and all sources of information cited have been duly acknowledged.

Anthony George Kachenko

Declared at
this day of
.....2008

**TO
MY PARENTS**

— ABSTRACT —

Soil contamination with heavy metal(loid)s is a major environmental problem that requires effective and affordable remediation technologies. The utilisation of plants to remediate heavy metal(loid)s contaminated soils has attracted considerable interest as a low cost *green* remediation technology. The process is referred to as *phytoremediation*, and this versatile technology utilises plants to *phytostabilise* and/or *phytoextract* heavy metal(loid)s from contaminated soils, thereby effectively minimising their threat to ecosystem, human and animal health. Plants that can accumulate exceptionally high concentrations of heavy metal(loid)s into above-ground biomass are referred to as *hyperaccumulators*, and may be exploited in phytoremediation, geobotanical prospecting and/or phytomining of low-grade ore bodies. Despite the apparent tangible benefits of utilising phytoremediation techniques, a greater understanding is required to comprehend the ecophysiological aspects of species suitable for phytoremediation purposes.

A screening study was instigated to assess phytoremediation potential of several fern species for soils contaminated with cadmium (Cd), chromium (Cr), copper (Cu), nickel (Ni), lead (Pb) and zinc (Zn). Hyperaccumulation was not observed in any of the studied species, and in general, species excluded heavy metal uptake by restricting their translocation into aboveground biomass. *Nephrolepis cordifolia* and *Hypolepis muelleri* were identified as possible candidates in phytostabilisation of Cu-, Pb-, Ni- or Zn-contaminated soils and *Dennstaedtia davallioides* appeared favourable for use in phytostabilisation of Cu- and Zn-contaminated soils. Conversely, *Blechnum nudum*, *B. cartilagineum*, *Doodia aspera* and *Calochlaena dubia* were least tolerant to most heavy metals and were classified as being least suitable for phytoremediation purposes

Ensuing studies addressed the physiology of arsenic (As) hyperaccumulation in a lesser known hyperaccumulator, *Pityrogramma calomelanos* var. *austroamericana*. The phytoremediation potential of this species was compared with that of the well known As hyperaccumulator *Pteris vittata*. Arsenic concentration of 3,008 mg kg⁻¹ dry weight (DW) occurred in *P. calomelanos* var. *austroamericana* fronds when exposed to 50 mg kg⁻¹ As without visual symptoms of phytotoxicities. Conversely, *P. vittata* was able to hyperaccumulate 10,753 mg As kg⁻¹ DW when exposed to 100 mg kg⁻¹ As without the onset

of phytotoxicities. In *P. calomelanos* var. *austroamericana*, As was readily translocated to fronds with concentrations 75 times greater in fronds than in roots. This species has the potential for use in phytoremediation of soils with As levels up to 50 mg kg⁻¹.

Localisation and spatial distribution of As in *P. calomelanos* var. *austroamericana* pinnule and stipe tissues was investigated using micro-proton induced X-ray emission spectrometry (μ -PIXE). Freeze-drying and freeze-substitution protocols (using tetrahydrofuran [THF] as a freeze-substitution medium) were compared to ascertain their usefulness in tissue preservation. Micro-PIXE results indicated that pinnule sections prepared by freeze-drying adequately preserved the spatial elemental distribution and tissue structure of pinnule samples. In pinnules, μ -PIXE results indicated higher As concentration than in stipe tissues, with concentrations of 3,700 and 1,600 mg As kg⁻¹ DW, respectively. In pinnules, a clear pattern of cellular localisation was not resolved whereas vascular bundles in stipe tissues contained the highest As concentration (2,000 mg As kg⁻¹ DW). Building on these μ -PIXE results, the chemical speciation of As in *P. calomelanos* var. *austroamericana* was determined using micro-focused X-ray fluorescence (μ -XRF) spectroscopy in conjunction with micro-focused X-ray absorption near edge structure (μ -XANES) spectroscopy. The results suggested that arsenate (As^V) absorbed by roots was reduced to arsenite (As^{III}) in roots prior to transport through vascular tissues as As^V and As^{III}. In pinnules, As^{III} was the predominant species, presumably as aqueous-oxygen coordinated compounds. Linear least-squares combination fits of μ -XANES spectra showed As^{III} as the predominant component in all tissues sampled. The results also revealed that sulphur containing thiolates may, in part sequester accumulated As.

The final aspect of this thesis examined several ecophysiological strategies of Ni hyperaccumulation in *Hybanthus floribundus* subsp. *floribundus*, a native Australian perennial shrub species and promising candidate in phytoremediation of Ni-contaminated soils. Micro-PIXE analysis revealed that cellular structure in leaf tissues prepared by freeze-drying was adequately preserved as compared to THF freeze-substituted tissues. Elemental distribution maps of leaves showed that Ni was preferentially localised in the adaxial epidermal tissues and leaf margin, with concentration of 10,000 kg⁻¹ DW in both regions. Nickel concentrations in stem tissues obtained by μ -PIXE analysis were lower than in the leaf tissues (1,800 mg kg⁻¹ vs. 7,800 mg kg⁻¹ DW, respectively), and there was no clear pattern of

compartmentalisation across different anatomical regions. It is possible that storage of accumulated Ni in epidermal tissues may provide Ni tolerance to this species, and may further act as a deterrent against herbivory and pathogenic attack. In *H. floribundus* subsp. *floribundus* seeds, μ -PIXE analysis did not resolve a clear pattern of Ni compartmentalisation and suggests that Ni was able to move apoplastically within the seed tissues.

The role of organic acids and free amino acids (low molecular weight ligands [LMW]) in Ni detoxification in *H. floribundus* subsp. *floribundus* were quantified using high performance liquid chromatography (HPLC) and ultra performance liquid chromatography (UPLC). Nickel accumulation stimulated a significant increase in citric acid concentration in leaf extracts, and based on the molar ratios of Ni to citric acid (1.3:1–1.7:1), citric acid was sufficient to account for approximately 50% of the accumulated Ni. Glutamine, alanine and aspartic acid concentrations were also stimulated in response to Ni hyperaccumulation and accounted for up to 75% of the total free amino acid concentration in leaf extracts. Together, these LMW ligands may complex with accumulated Ni and contribute to its detoxification and storage in this hyperaccumulator species.

Lastly, the hypothesis that hyperaccumulation of Ni in certain plants may act as an osmoticum under water stress (drought) was tested in context of *H. floribundus* subsp. *floribundus*. A 38% decline in water potential and a 68% decline in osmotic potential occurred between water stressed and unstressed plants, however, this was not matched by an increase in accumulated Ni. The results suggested that Ni was unlikely to play a role in osmotic adjustment in this species. Drought stressed plants exhibited a low water use efficiency which might be a conservative ecophysiological strategy enabling survival of this species in competitive water-limited environments.

* * *

— ACKNOWLEDGEMENTS —

“A journey of a thousand miles begins with a single step”

Lao-tzu, Chinese Philosopher (604 BC –531 BC).

It must be said that when I first commenced my postgraduate studies, I was somewhat overwhelmed with the thought of several years of *original* research, extensive field studies, hours of laboratory analyses, conference presentations, manuscript submissions – the litany could go on for ever. However, with careful planning, sound advice and support from several remarkable people, it was possible to negotiate hurdles, maintain momentum and focus on the onerous tasks at hand. During my final year as an undergraduate student, I can clearly recall the Dean of the Faculty of Agriculture, Food and Natural Resources (FAFNR), Professor Les Copeland, encouraging students to apply for postgraduate research scholarships. In his address, he proceeded to say that from his own experience, postgraduate study was one of the best, yet challenging times in your life. To Professor Les Copeland, I would have to say that to this day, I wholeheartedly agree with you.

To Associate Professor Balwant Singh, you have always travelled above and beyond your duty as supervisor in all aspects of my candidature, and have at all times maintained committed and dedicated to my research endeavours. I sincerely thank you for initiating this project, advising and encouraging me, and most importantly, for maintaining a high level of contact with me throughout the years, particularly during your sabbatical in 2006. I would like to sincerely thank Dr. Naveen Bhatia who steered me towards researching the ecophysiology of hyperaccumulation and the fascinating world of histology and μ -PIXE spectroscopy. Naveen played an integral part in several aspects of this work, notably the choice of hyperaccumulating species to research. Naveen always provided enthusiasm, encouragement and tremendous support throughout all aspects of my research, particularly during times when I couldn't see the light.

“I am not discouraged, because every wrong attempt discarded is another step forward.”

Thomas Alva Edison, American Inventor (1847 –1931)

My sincere thanks to Dr. Markus Gräfe (University of Sydney) and Dr. Rainer Siegele (Australian Nuclear Science and Technology Association: ANSTO) who were ‘de facto’ supervisors, and at all times provided invaluable support, criticisms and guidance when I needed it the most. Both Balwant and Markus introduced me to the intriguing world of synchrotron science and I feel honoured to have worked with such passionate scientists, and to have had the opportunity to conduct a beamline experiment and visit the Australian Synchrotron. I thank Dr. Rainer Siegele who bent over backwards to assist me with my μ -PIXE studies and made me feel welcome each and every visit to ANSTO. Rainer always had an answer to every question I threw at him, and at all times was enthusiastic and dedicated towards my studies. I would also like to thank Dr. David Cohen and Dr. Mihail Ionescu (ANSTO) who also made life a lot easier for me during my many ANSTO visits.

The bulk of this research would not have been possible without generous funding from several sources. I would like to acknowledge the support of the University of Sydney (USYD) for offering me a Commonwealth of Australia, Australian Postgraduate Award scholarship, and to the FAFNR for providing financial support. I also wish to acknowledge financial assistance from the Australian Institute of Nuclear Science and Engineering (AWARD No. AINGRA 05150 and 06160) and the Australian Institute of Agricultural Science & Technology Drought Research Fund. I wish to thank the Australian Synchrotron Research Program, for enabling me to travel to the Advanced Photon Source, Chicago, USA to conduct my beamline experiments. Lastly, I wish to acknowledge the U. S. Department of Energy, Office of Science, Office of Basic Energy Sciences, for funding my beam time.

I am indebted to the support of several people, who at some stage along the way provided much needed encouragement and/or support. To Mr. George and Mrs. Valerie Sonter from Sonters Fern Nurseries, thank you for introducing me to the world of fern propagation, showing me around your nursery, and supplying me with hundreds of sporelings. To Marilyn Sprague from Goldfields Revegetation Nursery, Mandurang, Victoria, thank you for your time in the field, providing me with your commentary on all things ‘native’ and supplying me with *Hybanthus* cuttings. To Associate Professor Nanjappa Ashwath from Central Queensland University, thank you for accompanying me to Mt. Morgan Gold Mine and assisting with field work. I wish to thank the Electron Microscope Unit for assistance with specimen preparation, particularly Ms. Emine Korkmaz, Dr. Louise Cole, Ms. Anne Simpson and Mr. Tony Romeo. I would also like to extend my gratitude to Mrs. Carol Campbell for

assisting me with anatomical interpretations of plant material and Dr. Edith Lees for providing constructive comments on this thesis. Thanks also goes to Dr. Steve Heald and Dr. Matt Newville (Advanced Photon Source, Argonne National Laboratory, Illinois, United States of America) and Dr. Euan Smith (University of South Australia, Adelaide) for assisting with various aspects of my synchrotron experiments. Special thanks to Mr. Bernie McInerney and Mr. Leon McQuade from the Australian Proteome Analysis Facility, Macquarie University, and Mr Malcolm Nobel from the University of New South Wales for sample analyses.

To the dedicated technical staff who assisted me at some stage along the way, my warmest appreciation. You are the skeleton that supports research and without your support, research would falter. In particular, I wish to thank Ms Iona György (Aunty I), who “*at the drop of a hat*” kindly offered her expertise whenever it was ‘demanded’, and was a friend more than a colleague. Thank you to Mr. Colin Bailey, Mr. Kevin McLauchlan, Mrs. Jarka Geisler and Ms. Nazaneen Soran for your technical assistance and support. Thanks also go to Mr. Tom Savage for his invaluable assistance in ICP-AES analyses, and to Ms. Maryann Ebsworth and Dr. Mick O’Neill, who provided much needed statistical advice. A big thank you to the administration staff, Ms. Pamela Stern, Ms. Prue Winkler, Ms. Fortunée Cantrell, Mr. Kyle Kiefer, Ms. Nancy Cheng and Ms. Pamela Brass who like the technical staff, provided me with overwhelming levels of logistical support throughout the course of my study.

During my time at USYD, I was provided with ample opportunity to get involved in the postgraduate community (and university politics) at both faculty and university levels. Thank you to the university bureaucracy for providing me with this experience, and a thank you goes to all those intriguing people who shed light on the *inner mechanisms* of university politics. To my fellow comrades in arms, it has truly been an amazing experience and I am glad that I shared this chapter in my life with you – all the very best in your future endeavours. The lunches and coffees have been a pleasant distraction and a superb chance to escape Room 227 (the dungeon) of Ross Street. To Dr. Prashant Srivastava and Dr. Ghulam Mustafa who helped me stand on my own two feet and showed me the ropes from day one, thank you. To all of Balwants past and present students, who made lab work fun and office work enjoyable, and I sincerely thank you for your camaraderie over the years. To the Panebianco family from

Ralph's Café, Archie and Steve, my thanks for all the laughs and good times, for the mouth watering food and exceptional coffees – 'bit of this.....bit of that'.

I wish to acknowledge the tremendous support from my family, particularly my sister Therese, who has always stood by me and given nothing but encouragement and praise. To all my friends, who have supported my studies over the years, thank you. I will no longer have to water plants on Saturday nights and on public holidays ever again (here's hoping). My passion for science, particularly biology began in high school, when Mrs. Margaret Shepherd captivated me by making the subject, interesting and thoroughly enjoyable. In particular, I wish to acknowledge Mr. Jim and Mrs. Jann Cloros (and George) and the EO crew, particularly Mr. Mike Mehigan and Ms. Susan Potthurst who have always offered support, friendship and shown interest in my affairs – thank you. In different ways, you have all taught me that, "When there is no vision, the people perish" (Proverbs 29:18).

And finally, I would like to convey my deepest love and heartfelt thanks to my parents who taught me that I can do all things through Christ, who has provided me with great strength and has sustained me throughout these challenging times. Mum and Dad, you have always told me to believe in myself and over the past 26 years and have bent over backward to provide me with a rich and fulfilling upbringing and a sound education. You instigated my passion for the great outdoors, the environment and all things horticultural. I fondly remember your encouraging words, in particular reaffirming that:

"Genius is one percent inspiration, ninety-nine percent perspiration"

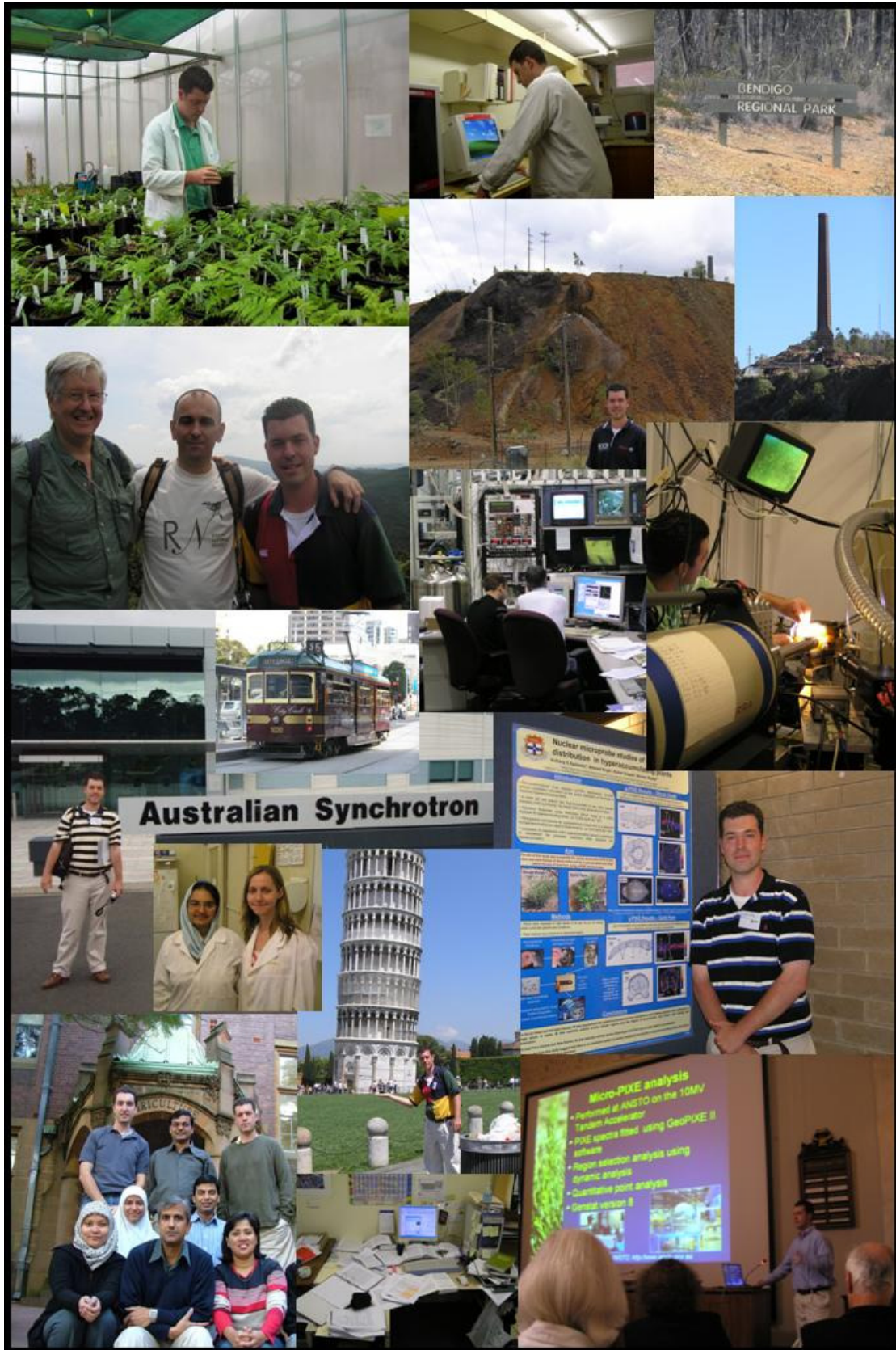
Thomas Alva Edison, American Inventor (1847–1931)

I thank you both for all you have sacrificed and for coping with my rollercoaster of ups and downs during the course of my studies. I can say that this experience had been a rich and rewarding one from which I have learnt that:

"The three great essentials to achieve anything worth while are, first, hard work; second, stick-to-itiveness; third, common sense."

Thomas Alva Edison, American Inventor (1847–1931)

— PICTORIAL TRAVELOGUE —



— PUBLICATIONS —

Refereed scientific journals (Published)

1. Kachenko AG, Singh B, Bhatia NP (2007) Heavy metal tolerance in common fern species. *Australian Journal of Botany* **55**, 63–73.
2. Kachenko AG, Bhatia NP, Singh B, Siegele R (2007) Arsenic hyperaccumulation and localization in the pinnule and stipe tissues of the gold-dust fern (*Pityrogramma calomelanos* (L.) Link var. *austroamericana* (Domin) Farw.) using quantitative micro-PIXE spectroscopy. *Plant and Soil* **300**, 207–219.
3. Kachenko AG, Singh B, Bhatia NP, Siegele R (2008) Quantitative elemental localisation in leaves and stems of nickel hyperaccumulating shrub *Hybanthus floribundus* subsp. *floribundus* using micro-PIXE spectroscopy. *Nuclear Instruments & Methods in Physics Research B* **266**, 667–676.
4. Siegele R, Kachenko AG, Bhatia NP, Wang YD, Ionescu M, Singh B, Baker AJM, Cohen DD (2008) Localisation of trace metals in metal-accumulating plants using μ -PIXE. *X-Ray Spectrometry* **37**, 133–136.
5. Kachenko AG, Siegele R, Bhatia NP, Singh B, Ionescu M (2008) Evaluation of specimen preparation techniques for micro-PIXE localisation of elements in hyperaccumulating plants. *Nuclear Instruments and Methods in Physics Research Section B* **266**, 1598–1604.

Refereed scientific journals (In preparation/submitted)

1. Kachenko AG, Gräfe, M, Singh B, Heald, S (2008) Arsenic speciation in hyperaccumulating *Pityrogramma calomelanos* var. *austroamericana* using X-ray absorption spectroscopy. *Environmental Science & Technology*. **Submitted**
2. Kachenko AG, Bhatia NP, Siegele R, Walsh KB, Singh B (2008) Nickel, zinc and cadmium localisation in seeds of metal hyperaccumulators using μ -PIXE spectroscopy. *Nuclear Instruments and Methods in Physics Research Section B*. **Submitted**
3. Siegele R, Kachenko AG, Ionescu M, Cohen DD (2008) Improved resolution and sensitivity on the ANSTO microprobe and it's application to PIXE. *Nuclear Instruments and Methods in Physics Research Section B*. **Submitted**
4. Kachenko AG, Singh B, Bhatia NP (2008) The role of low molecular weight ligands in nickel hyperaccumulation in *Hybanthus floribundus* subsp. *floribundus*. *Planta*. **In preparation**
5. Kachenko AG, Singh B, Bhatia NP (2008) A role for nickel in drought resistance in water-stressed *Hybanthus floribundus* subsp. *floribundus*. *Annals of Botany*. **In preparation**

Full conference papers (unrefereed)

1. Kachenko A G, Siegele R, Bhatia N P and Singh B (2007) Comparison of specimen preparation techniques for localisation of spatially distributed metal(loid)s in leaves of two hyperaccumulating plants. Proceedings of the 18th International Conference on Ion Beam Analysis. Hyderabad; India; September 23–28.
2. Kachenko AG, Singh B, Siegele R and Bhatia N P (2007) Nuclear microprobe studies of metal(loid) distribution in hyperaccumulating plants. Proceedings of the 15th AINSE Conference on Nuclear and Complementary Techniques of Analysis & 10th Vacuum Society of Australia Congress. Melbourne; Australia; November 21–23.
3. Siegele R, Kachenko AG, Wang YD, Ionescu M, Bhatia NP and Cohen DD (2007) Localisation of trace metals in metal-accumulating plants using μ -PIXE. Proceedings of the 15th AINSE Conference on Nuclear and Complementary Techniques of Analysis & 10th Vacuum Society of Australia Congress. Melbourne; Australia; November 21–23.
4. Siegele R, Kachenko AG, Bhatia NP, Wang YD, Ionescu M, Singh B, Baker, AJM and Cohen DD (2007) Localisation of trace metals in metal-accumulating plants using μ -PIXE. Proceedings of the 11th International Conference on Particle-Induced X-Ray Emission and its Analytical Applications. Puebla; Mexico; May 25–29.

Conference abstracts/posters (unrefereed)

1. Kachenko AG, Singh B, Bhatia NP, Siegele R (2006) Localisation & quantification of nickel in leaf and stem tissues of *Hybanthus floribundus* var. *floribundus* using micro-PIXE. Presented at the Fifth International Conference on Serpentine Ecology. Siena, Italy, May 9–13.
2. Kachenko AG, Singh B, Bhatia NP (2006) Phytostabilisation of toxic metals in contaminated soils using Australian native ferns. Presented at the Connect SUPRA Postgraduate Conference. Sydney; Australia; September 28–29.
3. Kachenko AG, Bhatia NP, Singh B, Siegele R (2006) Localisation & quantification of arsenic in *Pityrogramma calomelanos* (L.) Link var. *austroamericana*. Presented at the Faculty of Agriculture, Food and Natural Resources Symposium: New Horizons in Agricultural Research: Postgraduate Innovations. Sydney; Australia; November 24.
4. Kachenko AG, Gräfe M, Singh B and Heald SM (2007) Arsenic speciation in hyperaccumulating gold-dust fern using micro focussed X-ray absorption and X-ray fluorescence spectroscopies. ASRP/Australian Synchrotron Users Meeting. Melbourne; Australia; December 12–14.
5. Kachenko AG, Gräfe, M, Singh B, Heald, S (2008) Arsenic speciation in hyperaccumulating gold dust fern using micro focussed X-ray absorption spectroscopy. Presented at the Soils 2008 Conference. Palmerston North, New Zealand; December 1–5.

— TABLE OF CONTENTS —

ABSTRACT	iii
ACKNOWLEDGEMENTS	vi
PUBLICATIONS	xi
TABLE OF CONTENTS	xiii
LIST OF FIGURES	xxii
LIST OF TABLES	xxvi
ABBREVIATIONS	xxviii

CHAPTER 1: General introduction & background	1
1.1 GENERAL INTRODUCTION	1
1.2 HEAVY METAL(LOID)S IN THE SOIL ENVIRONMENT	3
1.2.1 Definition	3
1.2.2 Sources	4
1.2.3 Bioavailability	5
1.3 PLANT RESPONSE TO HEAVY METAL(LOID)S	8
1.3.1 Heavy metal(loid) tolerance	9
1.3.2 Plant tolerance strategies	9
1.3.3 Heavy metal(loid) hyperaccumulation	12
1.3.4 Serpentine soil: A hyperaccumulator host environment	13
1.3.5 Heavy metal(loid) hyperaccumulators in Australia	15
1.3.5.1 Background on Hybanthus floribundus	16
1.3.6 Ecological significance of hyperaccumulation	18
1.4 MECHANISMS OF HEAVY METAL(LOID) TOLERANCE	19
1.4.1 Avoidance tolerance mechanisms	20
1.4.1.1 Mycorrhizal associations	20
1.4.1.2 Rhizosphere effects	21
1.4.1.3 Cell wall	22
1.4.1.4 Plasma membrane	23
1.4.1.5 Metal efflux	24
1.4.2 Accumulation tolerance mechanisms	25
1.4.2.1 Plant Ligands	25
1.4.2.2 Localisation of heavy metal(loid)s in plant tissues	32
1.4.3 Heavy metal(loid) uptake and translocation in hyperaccumulators	38
1.5 REMEDIATION OF POLLUTED SOILS	40
1.5.1 Phytoremediation	41
1.5.2 Subgroups of phytoremediation	42
1.6 HEAVY METAL(LOID)S IN FERNS	44
1.6.1 Heavy metal(loid)s tolerance in ferns	44
1.6.2 Hyperaccumulating ferns	46
1.6.2.1 Background on Pityrogramma calomelanos var. austroamericana	48
1.7 AIMS AND OBJECTIVES	50
1.7.1 Rationale	50
1.7.2 Aims	51
1.7.3 Objectives	51

CHAPTER 2: Screening for heavy metal tolerance in common Australian fern species	53
ABSTRACT	53
2.1 INTRODUCTION	54
2.2 MATERIALS AND METHODS	56
2.2.1 <i>Selection of fern material</i>	56
2.2.2 <i>Greenhouse experiment</i>	56
2.2.3 <i>Chemical analysis</i>	57
2.2.4 <i>Statistical analysis</i>	58
2.3 RESULTS	58
2.3.1 <i>Fronde and root biomass</i>	58
2.3.2 <i>Heavy metal concentrations in the fronds and roots</i>	63
2.3.3 <i>Heavy metal accumulation</i>	67
2.3.4 <i>Heavy metal translocation by ferns</i>	69
2.4 DISCUSSION	70
2.5 CONCLUSION	74

CHAPTER 3: Evaluation of specimen preparation techniques for elemental localisation in hyperaccumulating tissues	75
ABSTRACT	75
3.1 INTRODUCTION	76
3.2 MATERIALS AND METHODS	78
3.2.1 <i>Selection of plant material</i>	78
3.2.1.1 <i>Hybanthus floribundus</i> subsp. <i>floribundus</i>	78
3.2.1.2 <i>Pityrogramma calomelanos</i> var. <i>austroamericana</i>	78
3.2.2 <i>Sample preparation</i>	79
3.2.2.1 <i>Freeze-drying</i>	79
3.2.2.2 <i>Chemical analysis</i>	79
3.2.2.3 <i>Freeze-substitution using tetrahydrofuran</i>	80
3.2.3 <i>Micro-PIXE setup</i>	80
3.2.4 <i>Statistical analysis</i>	82
3.3 RESULTS	82
3.3.1 <i>Micro-PIXE analysis</i>	82
3.2.3.1 <i>Hybanthus floribundus</i> subsp. <i>floribundus</i>	82
3.2.3.2 <i>Pityrogramma calomelanos</i> var. <i>austroamericana</i>	85
3.4 DISCUSSION	87
3.3 CONCLUSION	89

CHAPTER 4:	Arsenic hyperaccumulation and localisation in	91
	<i>Pityrogramma Calomelanos var. austroamericana</i>	
<hr/>		
ABSTRACT		91
4.1 INTRODUCTION		92
4.2 MATERIALS AND METHODS		94
4.2.1 Selection of fern material		94
4.2.2 Experimental conditions		94
4.2.3 Chemical analysis		94
4.2.4 Micro-PIXE study		95
4.2.4.1 Light microscopy		95
4.2.4.2 Sample preparation for micro-PIXE analysis		95
4.2.4.3 Micro-PIXE analysis		97
4.2.5 Statistical analysis		97
4.3 RESULTS		97
4.3.1 Arsenic accumulation		97
4.3.2 Frond and root biomass		97
4.3.2 Light microscopy		98
4.3.2.1 Pinnule anatomy		98
4.3.2.2 Stipe anatomy		99
4.3.4 Micro-PIXE analysis		101
4.4 DISCUSSION		108
4.5 CONCLUSION		112

CHAPTER 5: Quantitative nickel localisation in leaf, stem and seed tissues of <i>Hybanthus floribundus</i> subsp. <i>floribundus</i>	113
<hr/>	
ABSTRACT	113
5.1 INTRODUCTION	114
5.2 MATERIALS AND METHODS	116
5.2.1 <i>Selection of plant material</i>	116
5.2.2 <i>Sample preparation</i>	116
5.2.3 <i>Light microscopy</i>	116
5.2.4 <i>Micro-PIXE setup</i>	116
5.2.5 <i>Statistical analysis</i>	116
5.3 RESULTS	117
5.3.1 <i>Light microscopy</i>	117
5.3.1.1 <i>Leaf anatomy</i>	117
5.3.1.2 <i>Stem anatomy</i>	117
5.3.1.3 <i>Seed anatomy</i>	117
5.3.2 <i>Micro-PIXE analysis</i>	119
5.4 DISCUSSION	128
5.5 CONCLUSION	131

CHAPTER 6:	Arsenic speciation in tissues of the hyperaccumulator	133
	<i>P. calomelanos var. austroamericana</i>	

ABSTRACT	133
6.1 INTRODUCTION	134
6.2 MATERIALS AND METHODS	135
6.2.1 <i>Selection of plant material</i>	135
6.2.2 <i>Total arsenic determination by ICP-AES</i>	136
6.2.3 <i>Micro-X-ray absorption spectroscopy (μ-XAS)</i>	136
6.2.3.1 <i>Sample preparation</i>	136
6.2.3.2 <i>Micro-X-ray fluorescence imaging (μ-XRF)</i>	136
6.2.3.3 <i>Micro-X-ray absorption near edge structure analysis (μ-XANES)</i>	137
6.2.4 <i>Data analysis</i>	138
6.3 RESULTS	141
6.3.1 <i>Arsenic concentration in ferns</i>	141
6.3.2 <i>Micro-X-ray fluorescence imaging</i>	142
6.3.3 <i>Micro-X-ray absorption near edge structure analysis (μ-XANES)</i>	143
6.4 DISCUSSION	152
6.5 CONCLUSION	156

CHAPTER 7: The role of low molecular weight ligands in nickel hyperaccumulation in <i>H. floribundus</i> subsp. <i>floribundus</i>	157
ABSTRACT	157
7.1 INTRODUCTION	158
7.2 MATERIALS AND METHODS	160
7.2.1 <i>Greenhouse study</i>	160
7.2.1.1 Selection of plant material	160
7.2.1.2 Chemical analysis	161
7.2.2 <i>Organic acid and free amino acid study</i>	161
7.2.2.1 Tissue extraction	161
7.2.2.2 Organic acid analysis	161
7.2.2.3 Amino acid analysis	162
7.2.3 <i>Statistical analysis</i>	163
7.3 RESULTS	164
7.3.1 <i>Greenhouse study</i>	164
7.3.1.1 Biomass	164
7.3.1.2 Nickel concentration in tissues	164
7.3.1.3 Nickel accumulation	165
7.3.2 <i>Organic acid and free amino acid study</i>	167
7.3.2.1 Nickel concentration in shoot extracts	167
7.3.2.2 Organic acids	167
7.3.2.2 Amino acids	170
7.4 DISCUSSION	173
7.4.1 <i>Organic acids</i>	173
7.4.2 <i>Free amino acids</i>	175
7.5 CONCLUSION	177

CHAPTER 8:	A role for nickel in drought resistance in water-stressed	179
	<i>H. floribundus</i> subsp. <i>floribundus</i>	
<hr/>		
ABSTRACT		179
8.1 INTRODUCTION		180
8.2 MATERIALS AND METHODS		182
8.2.1 <i>Plant material and soil preparation</i>		182
8.2.2 <i>Soil analysis</i>		183
8.2.3 <i>Experimental conditions</i>		186
8.2.4 <i>Plant water relation parameters</i>		186
8.2.4.1 <i>Water potential (Ψ_w)</i>		186
8.2.4.2 <i>Osmotic potential (Ψ_π)</i>		187
8.2.4.3 <i>Relative water content (RWC)</i>		187
8.2.4.4 <i>Gas exchange</i>		188
8.2.4.5 <i>Water-use efficiency (WUE)</i>		188
8.2.4.6 <i>Carbon isotope discrimination</i>		188
8.2.4.7 <i>Chemical analysis</i>		189
8.2.3 <i>Statistical analysis</i>		189
8.3 RESULTS		190
8.3.1 <i>Biomass</i>		190
8.3.2 <i>Nickel concentration and accumulation</i>		190
8.3.3 <i>Water relation parameters</i>		192
8.4 DISCUSSION		194
8.5 CONCLUSION		197
CHAPTER 9:	Conclusions and future research	199
<hr/>		
BIBLIOGRAPHY		205
<hr/>		
APPENDICES		229
<hr/>		

— LIST OF FIGURES —

CHAPTER 1

Figure 1.1	A model for depicting available heavy metal(loid)s in soil adapted from Morel (1997).....	6
Figure 1.2	A dose response curve for essential (solid line) and non-essential (broken line) elements in plants. Modified after Morel (1997).....	9
Figure 1.3	Plant tolerance strategies in response to increasing soil heavy metal(loid) concentrations, modified from Baker (1981; a, c, e). Corresponding plant growth characteristics in response to increasing soil characteristics, are also presented (Bhatia, 2003; b, d, f).....	11
Figure 1.4	A typical serpentine site (Nature Reserve of Monterufoli) in Tuscany, Italy showing lack of vegetation cover and steep, rocky slopes (May, 2006).....	14
Figure 1.5	A typical <i>Hybanthus floribundus</i> subsp. <i>floribundus</i> in natural habitat in Bendigo Regional Park, South Mandurang, Victoria.....	17
Figure 1.6	An overview of possible mechanisms involved in heavy metal(loid) tolerance. Modified after Marschner (1997).....	20
Figure 1.7	Chemical structure of (a) phytochelatins, (b) histidine and (c) citric acid adapted from Callahan <i>et al.</i> 2006.....	26
Figure 1.8	Naturally occurring populations of <i>Pityrogramma calomelanos</i> var. <i>austroamericana</i> growing along the Dee River, Mount Morgan, Queensland (a-d).....	49

CHAPTER 2

Figure 2.1	Fronnd dry weight (g) of different fern species with various heavy metal treatments after 20 weeks of growth, (a) Cd, (b) Cr, (c) Cu, (d) Ni, (e) Pb and (f) Zn	61
Figure 2.2	Root dry weight (g) of different fern species with various heavy metal treatments after 20 weeks of growth, (a) Cd, (b) Cr, (c) Cu, (d) Ni, (e) Pb and (f) Zn	62
Figure 2.3	(a) Stunted growth in <i>Nephrolepis cordifolia</i> after exposure to increasing levels of Cd. (b) Stunted growth in <i>Hypolepis muelleri</i> after 20 weeks exposure to increasing levels of Cd (death occurred in all replicates exposed to 500 mg kg ⁻¹ Cd). (c) Severely stunted growth in <i>Blechnum nudum</i> after 4 weeks exposure to 500 mg kg ⁻¹ Cr. (d) Stunted growth and necrotic pinnae in <i>Pellaea falcata</i> after 14 weeks exposure to 500 mg kg ⁻¹ Zn.....	63
Figure 2.4	Concentrations (mg kg ⁻¹ DW) of Cd (a), Cr (b), Cu (c) Ni (d), Pb (e) and Zn (f) in fronds of different fern species after 20 weeks of growth.....	65
Figure 2.5	Concentrations (mg kg ⁻¹ DW) of Cd (a), Cr (b), Cu (c) Ni (d), Pb (e) and Zn (f) in roots of different fern species after 20 weeks of growth.....	66
Figure 2.6	Accumulation (µg plant ⁻¹) of Cd (a), Cr (b), Cu (c), Ni (d), Pb (e) and Zn (f) in different fern species after 20 weeks of growth.....	68

CHAPTER 3

Figure 3.1	(a) Nuclear microprobe end station. The target chamber is indicated by the red arrow. (b) Inside the target chamber. The Ge detector is indicated by the yellow arrow.....	81
Figure 3.2	Average concentration (± standard error) of elements in <i>Hybanthus floribundus</i> subsp. <i>floribundus</i> leaf (a) and <i>Pityrogramma calomelanos</i> var. <i>austroamericana</i> pinnule (b) after ICP-AES analysis of bulk tissue and µ-PIXE analysis of freeze-dried and freeze-substituted (tetrahydrofuran) cross-sections.....	83
Figure 3.3	Elemental maps of Ni in a high pressure frozen, tetrahydrofuran freeze-substituted (b) and hand sectioned, cryo-fixed freeze-dried (d) leaf cross-section of <i>Hybanthus floribundus</i> subsp. <i>floribundus</i> sandwiched between Formvar films after 20 weeks of Ni exposure. A typical optical micrograph of a freeze-substituted (a) and freeze-dried (c) <i>H. floribundus</i> subsp. <i>floribundus</i>	84
Figure 3.4	Elemental maps of As in a high pressure frozen, tetrahydrofuran freeze-substituted (b) and hand sectioned, cryo-fixed freeze-dried (d) pinnule cross-section of <i>Pityrogramma calomelanos</i> var. <i>austroamericana</i> sandwiched between Formvar films after 20 weeks of As exposure. A typical optical micrograph of a freeze-substituted (a) and freeze-dried (c) <i>P. calomelanos</i> var. <i>austroamericana</i> leaf is also presented.....	86

CHAPTER 4

- Figure 4.1** Arsenic phytotoxicities in *P. calomelanos* var. *austroamericana* ferns exposed to As treatments for 20 weeks. Phytotoxicities were not observed in ferns exposed to 0 mg As kg⁻¹ (a) and 50 mg As kg⁻¹ (b) treatments. Severely stunted growth and necrotic pinnules were observed in ferns exposed to 100 mg As kg⁻¹ (c) and 500 mg As kg⁻¹ (d). 96
- Figure 4.2** Frond (a) and root (b) As concentration (mg kg⁻¹) in *Pityrogramma calomelanos* var. *austroamericana* and *Pteris vittata* and, frond (c) and root (d) dry weight (g plant⁻¹) of *Pityrogramma calomelanos* var. *austroamericana* and *Pteris vittata* after 20 weeks of growth. 98
- Figure 4.3** Light micrograph of transversely cut resin embedded As-treated pinnule (a) and stipe (c) section (1 µm, magnification × 40) of *Pityrogramma calomelanos* var. *austroamericana* stained with toluidine blue. Insert (b) details (magnification × 200) the cross section pinnae anatomy and insert (d) details (magnification × 200) the stele. 100
- Figure 4.4** Typical µ-PIXE spectra obtained for a pinnule (a) and stipe (b) sections of a *P. calomelanos* subsp. *austroamericana*. Note the main As K_α peak at 10.530 keV, and the secondary As K_β peak at 11.722 KeV. Peaks for other elements are also indicated. 101
- Figure 4.5** A representative optical micrograph (a), and elemental maps showing distribution of As (b), Ca (c) and K (d) in a hand sectioned, cryo-fixed freeze-dried pinnule cross-section of *Pityrogramma calomelanos* var. *austroamericana* sandwiched between Formvar films after 20 weeks of exposure to 50 mg As kg⁻¹. Adjoining each elemental map are quantitative point analysis (QPA) profiles derived from the µ-PIXE analysis across a typical area transect outlined in green on the corresponding map. 103
- Figure 4.6** A typical optical micrograph (a), and elemental maps of As (b), Ca (c) and K (d) in a stipe cross-section of *Pityrogramma calomelanos* var. *austroamericana* sandwiched between Formvar films after 20 weeks of exposure to 50 mg As kg⁻¹. Adjoining each elemental map are quantitative point analysis (QPA) profiles derived from the µ-PIXE analysis across a typical area transect outlined in green on the corresponding map. 106

CHAPTER 5

- Figure 5.1** Light micrograph of Ni-treated leaf (a) and stem (b) sections (1 µm, magnification × 40) of *Hybanthus floribundus* subsp. *floribundus*. The regions distinguished by broken lines represent leaf margin (1); mid-blade (2) and midrib (3). 118
- Figure 5.2** Typical µ-PIXE spectra of a *H. floribundus* subsp. *floribundus* leaf (a), stem (b) and seed (c). Note the main Ni K_α peak at 7.471 keV, and the secondary Ni K_β peak at 8.263 KeV. Peaks for other elements are also indicated. 120
- Figure 5.3** A representative optical micrograph (a), and elemental maps showing distribution of Ni (b), Ca (c) and K (d) in a hand sectioned, cryo-fixed freeze-dried leaf cross-section of *H. floribundus* subsp. *floribundus* sandwiched between Formvar films after 20 weeks of exposure to 1,500 mg kg⁻¹ Ni. Adjoining each elemental map are quantitative point analysis (QPA) profiles derived from the µ-PIXE analysis across a typical area transect outlined in green on the corresponding map. 121
- Figure 5.4** A representative optical micrograph (a), and elemental maps showing distribution of Ni (b), Ca (c) and K (d) in a hand sectioned, cryo-fixed freeze-dried stem cross-section of *H. floribundus* subsp. *floribundus* sandwiched between Formvar films after 20 weeks of exposure to 1,500 mg kg⁻¹ Ni. Adjoining each elemental map are quantitative point analysis (QPA) profiles derived from the µ-PIXE analysis across a typical area transect outlined in green on the corresponding map. 124
- Figure 5.5** A representative optical micrograph (a), and elemental maps showing distribution of Ni (b), Ca (c) and K (d) in an air-dry seed longitudinal-section of *H. floribundus* subsp. *floribundus*. Adjoining each elemental map are quantitative point analysis (QPA) profiles derived from the µ-PIXE analysis across a typical area transect outlined in green on the corresponding map. 127

CHAPTER 6

- Figure 6.1** Arsenic K near-edge spectra of aqueous arsenite (As^{III} ; 6.7 mM NaHAsO_2) and arsenate (As^{V} ; 5 mM $\text{Na}_2\text{HAsO}_4 \cdot 7\text{H}_2\text{O}$) model compounds. Where y is the whiteline energy of As^{III} (11872.2 eV) and z is the point of inflection where As^{III} crossed the As^{V} whiteline energy (11875.5 eV). Vertical lines are drawn at 11872.2 eV and 11875.5 eV to indicate the position of the absorption edge for arsenite (As^{III}) and arsenate (As^{V}), respectively. **139**
- Figure 6.2** *Pityrogramma calomelanos* var. *austroamericana* ferns exposed to 0 and 50 mg kg^{-1} As^{V} for 10 weeks. **141**
- Figure 6.3** Concentration of As in (a) the pinnae, (b) stipe (○) and rachis (●) tissues along the axis of three *Pityrogramma calomelanos* var. *austroamericana* fronds exposed to 50 mg kg^{-1} As for 10 weeks. Data points are indicated on the adjoining optical image. **142**
- Figure 6.4** Qualitative As K-edge μ -XRF images of *Pityrogramma calomelanos* var. *austroamericana* tissues exposed to 50 mg kg^{-1} As^{V} for 10 weeks. Tip of pinnule (A–C), two views of costa (D–I), rachis (J–L) and stipe (M–O) each showing optical micrograph and the relative concentration of arsenite and arsenate. The μ -XRF signals were collected at 25 μm step size. The normalised intensity scale is arbitrary with the black and white corresponding to the lowest and highest relative concentrations, respectively. **145**
- Figure 6.5** Qualitative As K-edge μ -XRF images of *Pityrogramma calomelanos* var. *austroamericana* tissues exposed to 5 mM As^{V} for 40 h. Uncoiling crozier (A–C), costa (D–F), stipe (G–I) and root (J–L) each showing optical micrograph and the relative concentration of arsenite and arsenate. The μ -XRF signals were collected at 25 μm step size. The normalised intensity scale is arbitrary with the black and white corresponding to the lowest and highest relative concentrations, respectively. **146**
- Figure 6.6** Arsenic K-edge μ -XANES spectra of model compounds and bulk *P. calomelanos* var. *austroamericana* freeze-dried pinnule and stipe/rachis tissues. Vertical lines drawn at 11872.2 eV and 11875.5 eV indicate the position of the whitelines for arsenite (As^{III}) and arsenate (As^{V}), respectively. **147**
- Figure 6.7** Arsenic K-edge μ -XANES spectra for various regions of *P. calomelanos* var. *austroamericana* frond tissues exposed to 50 mg kg^{-1} As^{V} for 10 weeks. Vertical lines drawn at 11872.2 eV and 11875.5 eV indicate the position of the whitelines for arsenite (As^{III}) and arsenate (As^{V}), respectively. **148**
- Figure 6.8** Arsenic K-edge μ -XANES spectra for five regions of *P. calomelanos* var. *austroamericana* exposed to 5 mM As^{V} for 40 h. Vertical lines drawn at 11872.2 eV and 11875.5 eV indicate the position of the whitelines for arsenite (As^{III}) and arsenate (As^{V}), respectively. **149**
- Figure 6.9** Arsenic K-edge μ -XANES fits of (a) pinnule lamina and (b) root tissues of *P. calomelanos* var. *austroamericana*. Pinnule lamina from ferns exposed to 50 mg kg^{-1} As^{V} for 10 weeks and roots from ferns exposed to 5 mM As^{V} for 40 h. The results of these fits are presented in Table 6.4. Vertical lines drawn at 11872.2 eV and 11875.5 eV indicate the position of the whitelines for arsenite (As^{III}) and arsenate (As^{V}), respectively. **151**

CHAPTER 7

- Figure 7.1** Representative *Hybanthus floribundus* subsp. *floribundus* plants following 20 weeks exposure to various Ni concentrations (mg kg^{-1}). **165**
- Figure 7.2** (a) Dry weight, (b) Ni concentration and (c) Ni accumulation in root, stem and leaf tissues of *Hybanthus floribundus* subsp. *floribundus* at different Ni application rates after 20 weeks of growth. **166**
- Figure 7.3** Nickel concentration in 0.025 M HCl shoot extracts of *Hybanthus floribundus* subsp. *floribundus* at different Ni application rates after 20 weeks of growth. **167**
- Figure 7.4** Typical HPLC chromatogram of organic acids in a 0.025 M HCl shoot extract of *H. floribundus* subsp. *floribundus* following 20 weeks exposure to 2,000 mg kg^{-1} Ni. **168**
- Figure 7.5** Typical auto-scaled UPLC chromatogram of amino acids in a 0.025 M HCl *H. floribundus* subsp. *floribundus* shoot extract following 20 weeks exposure to 2000 mg kg^{-1} Ni. **170**
-

CHAPTER 8

Figure 8.1	A representative 3 × 3 m transect randomly selected for soil sampling in Bendigo Regional Park, South Mandurang, Victoria, Australia.	182
Figure 8.2	Moisture characteristic curve for the experimental soil used for the pot experiment.	185
Figure 8.3	Representative <i>Hybanthus floribundus</i> subsp. <i>floribundus</i> plants following 12 weeks exposure to 1,000 mg kg ⁻¹ Ni in soil at varying levels of water potential.	190
Figure 8.4	(a) Dry weight, (b) Ni concentration and (c) Ni accumulation in root and shoot tissues of <i>Hybanthus floribundus</i> subsp. <i>floribundus</i> exposed to 1,000 mg kg ⁻¹ Ni in soil at different levels of water potential.	191

— LIST OF TABLES —

CHAPTER 1

Table 1.1	Classification of heavy metals based on Lewis acidity adapted from Neiboer and Richardson (1980).....	4
Table 1.2	Heavy metal(loid) hyperaccumulating plants.	13
Table 1.3	Review of heavy metal(loid)s localisation studies in hyperaccumulating species.	34
Table 1.4	Advantages and disadvantages of phytoremediation adapted from Glass (1999) and Ghosh and Singh (2005).	42
Table 1.5	Review of confirmed As hyperaccumulating species.	47

CHAPTER 2

Table 2.1	Detection limits and wavelengths used for atomic absorption spectrometer (AAS) and graphite furnace atomic absorption spectrometer (GF-AAS) analyses.	58
Table 2.2	Results of two-way ANOVA showing probability (<i>P</i>) for biomass, heavy metal concentration and accumulation in ferns between populations, treatments and interaction between species and treatments.	59
Table 2.3	Survival rate (%) of the 10 ferns across all treatments of various heavy metals after 20 weeks of growth.	60
Table 2.4	Mean heavy metal translocation factors across all treatment levels (TF; concentration ratio of heavy metal in the frond to root) of the 10 fern species after 20 weeks of growth. The degree of heavy metal accumulation in harvestable biomass for each species is ranked according to its mean frond heavy metal uptake across the 50 and 100 mg kg ⁻¹ levels as denoted in parentheses.	69

CHAPTER 3

Table 3.1	Detection limits and wavelengths used for inductively coupled plasma-atomic emission spectrometer (ICP-AES) analysis.	80
Table 3.2	Average concentration of elements (mg kg ⁻¹ DW) in <i>Hybanthus floribundus</i> subsp. <i>floribundus</i> leaf cross-sections after freeze-drying and freeze-substitution with tetrahydrofuran.	85
Table 3.3	Average concentration of elements (mg kg ⁻¹ DW) in <i>Pityrogramma calomelanos</i> var. <i>austroamericana</i> pinnule sections after freeze-drying and freeze-substitution with tetrahydrofuran.	87

CHAPTER 4

Table 4.1	Average concentration of elements (mg kg ⁻¹ DW) within pinnule sections of <i>Pityrogramma calomelanos</i> var. <i>austroamericana</i> as determined following dynamic analysis of individually selected regions. The results are presented as means ± SE of three replicates.	104
Table 4.2	Average concentration (mean ± SE; <i>n</i> = 3) of elements along the length of As-treated freeze-dried pinnule sections of <i>Pityrogramma calomelanos</i> var. <i>austroamericana</i> following region selection analysis.	105
Table 4.3	Average concentration of elements (mg kg ⁻¹ DW) within stipe sections of <i>Pityrogramma calomelanos</i> var. <i>austroamericana</i> as determined following dynamic analysis of individually selected regions. The results are presented as means ± SE of three replicates.	107

CHAPTER 5

Table 5.1	Average concentration of elements (mg kg^{-1} DW) within leaf sections of <i>Hybanthus floribundus</i> subsp. <i>floribundus</i> as determined following dynamic analysis of individually selected regions. The results are presented as means \pm SE of three replicates.	122
Table 5.2	Average concentration (mean \pm SE; $n=3$) of elements along the length of Ni-treated freeze-dried leaf sections of <i>Hybanthus floribundus</i> subsp. <i>floribundus</i> following region selection analysis. ...	123
Table 5.3	Average concentration of elements (mg kg^{-1} DW) within stem sections of <i>Hybanthus floribundus</i> subsp. <i>floribundus</i> as determined following dynamic analysis of individually selected regions. The results are presented as means \pm SE of three replicates.	125
Table 5.4	Average concentration of elements (mg kg^{-1} DW) within seed sections of <i>H. floribundus</i> subsp. <i>floribundus</i> as determined following dynamic analysis of individually selected regions. The results are presented as means \pm SE of three replicate seeds.	126

CHAPTER 6

Table 6.1	Summary of As standards used in the study. Whiteline (peak of the absorption edge) positions are based on published literature.	138
Table 6.2	Principal component analysis of 60 normalised μ -XANES spectra.	143
Table 6.3	Target transformation results for model compounds.	144
Table 6.4	Linear least-square combination fits of μ -XANES spectra for As in bulk, freeze-dried materials and As exposed <i>Pityrogramma calomelanos</i> var. <i>austramericana</i> tissues. Fit results correspond to μ -XANES spectra plotted in Figures 6.7-6.9.	150

CHAPTER 7

Table 7.1	Limit of detection for each organic acid investigated using HPLC.	162
Table 7.2	Eluent gradients details of UPLC operation for tissue extract analysis.	164
Table 7.3	Concentration of organic acids (mg kg^{-1} DW) in 0.025 M HCl extract of <i>Hybanthus floribundus</i> subsp. <i>floribundus</i> shoot tissues at different levels of Ni after 20 weeks of growth.	169
Table 7.4	Correlation coefficients (r) between amino acids and Ni concentration in 0.025 M HCl extract and leaf and stem tissues.	171
Table 7.5	Concentration of amino acids (mg kg^{-1} DW) in 0.025 M HCl extract of <i>Hybanthus floribundus</i> subsp. <i>floribundus</i> shoots at different levels of Ni after 20 weeks of growth.	172

CHAPTER 8

Table 8.1	Important physical and chemical properties used for the pot experiment.	184
Table 8.2	Mean values of water potential (Ψ_w), osmotic potential (Ψ_π), relative water content (RWC), photosynthesis (A), transpiration (E), stomatal conductance (g_s), water-use deficiency (WUE) and carbon isotope discrimination (Δ) in <i>H. floribundus</i> subsp. <i>floribundus</i> plants grown in a soil spiked with $1,000 \text{ mg Kg}^{-1}$ Ni and exposed to different levels of water potentials ($-\text{kPa}$).	193

— ABBREVIATIONS —

AAS	atomic absorption spectrometer
AFA	abstract factor analysis
AM	arbuscular mycorrhiza
ANOVA	analysis of variance
ANSTO	Australian Nuclear Science and Technology Organisation
ANU	Australian National University
APS	Advanced Photon Source
AR	analytical reagent
BDL	below detection limit
CDF	cation diffusion facilitator
cDNA	complimentary deoxyribonucleic acid
CMT	computed-microtomography
Cys	cysteine
DA	dynamic analysis
DMA	dimethylarsenic acid
DPX	distrene, plasticiser, xylene
DTPA	diethylenetriamine pentaacetic acid
DW	dry weight
EC	electrical conductivity
ECO	ectomycorrhiza
EDTA	ethylenediaminetetraacetic acid
EDXA	energy dispersive X-ray analysis
EELS	electron energy loss spectroscopy
EXAFS	extended X-ray absorption fine structure
FAFNR	Faculty of Agriculture, Food and Natural Resources
GC-MS	gas chromatography-mass spectrometry
GF-AAS	graphite furnace atomic absorption spectrometer
Glu	glutamate
Gly	glycine
GSH	glutathione
HClO ₄	perchloric acid

HNO ₃	nitric acid
HPLC	high precision liquid chromatography
HSP	heat shock protein
ICP-AES	inductively coupled plasma-atomic emission spectrometry
IND	indicator value
IRT	iron-regulated transporter
LCF	linear least-squares combination fit
LMW	low molecular weight
LN ₂	liquid nitrogen
LS	level of significance
LSD	least significant difference
MDL	minimum detection limit
μ-PIXE	micro-proton induced X-ray emission
μ-XANES	micro-X-ray absorption near-edge structures
μ-XRF	micro-X-ray fluorescence
μ-XRS	micro-X-ray spectroscopy
MDL	minimum detection limit
MMA	methylarsonic acid
MT	metallothioneins
nano-SIMS	nano-secondary ion mass spectrometry
NIST-SRM	National Institute of Standards and Technology- Standard Reference Materials
NRAMP	natural resistance-associated macrophage protein
NSS	normalised sum-square
PC	phytochelatins
PCA	principal component analysis
PNC/XOR	Pacific Northwest. Consortium/X-ray Operations Research
QPA	quantitative point analysis
REML	restricted maximum likelihood
ROI	regions of interest
RSA	region selection analysis
RSD	relative standard deviation
RWC	relative water content
SD	standard deviation

SE	standard error
SS	sum-square
STEM	scanning transmission electron microscopy
TF	translocation factor
THF	tetrahydrofuran
TT	target transformation
UPLC	ultra performance liquid chromatography
USEPA	United States Environmental Protection Agency
VAM	vesicular arbuscular mychorrhiza
WUE	water use efficiency
XAS	X-ray absorption spectroscopy
ZIP	zipper interacting protein
ZRT	zinc regulated transporter